Adolescent reference values for MR-derived biventricular strain obtained using feature-tracking and myocardial tagging

Carlos Real, MD[1,2], Rocío Párraga, MD[1,2], Ernesto González-Calvo, MD[1,2], Eva Gutiérrez-Ortiz, MD[1,2], ,Raquel Díaz-Muñoz, NP PhD[3], Javier Sánchez-González, PhD[4], María Beneito-Durá, BS[1], Jesús Martínez-Gómez, MS[1]; Gonzalo Pizarro, MD, PhD[1,5,6], Inés García-Lunar, MD[1,6,7], PhD, Rodrigo Fernández-Jiménez, MD, PhD[1,2,7,8]

[1]Centro Nacional de Investigaciones Cardiovasculares, Madrid, Spain
[2]Department of Cardiology, Hospital Universitario Clínico San Carlos, Madrid, Spain
[3]Centro Nacional de Epidemiología, Instituto de Salud Carlos III, Madrid, Spain
[4]Philips Healthcare Spain, Madrid, Spain
[5]Department of Cardiology, Hospital Ruber Juan Bravo Quironsalud UEM, Madrid, Spain
[6]CIBER de enfermedades cardiovasculares (CIBER-CV), Madrid, Spain
[7]Department of Cardiology, Hospital Universitario La Moraleja, Madrid, Spain
[8]Instituto de Investigación Sanitaria del Hospital Clínico San Carlos, IdISSC, Madrid, Spain

Address for correspondence:
Rodrigo Fernández-Jiménez, MD, PhD. Centro Nacional de Investigaciones Cardiovasculares (CNIC). Calle Melchor Fernández Almagro, 3, 28029, Madrid, Spain. Tel: (+34) 914531200. Fax: (+34) 914531265. E-mail: rodrigo.fernandez@cnic.es

Ackowledgments:
The authors would like to thank the SHE Foundation–intellectual owner of the SI! Program–and its collaborators, and are indebted to the adolescents and their families who participated in this study. Simon Bartlett (CNIC) provided English editing.

Grant support:
The EnIGMA (Early ImaGing Markers of unhealthy lifestyles in Adolescents) study was funded by the Instituto de Salud Carlos III (ISCIII) through the project "PI19/01704" and co-funded by the European Union. J.M-G is a recipient of grant FPU21/04891 (Ayudas para la formación de profesorado universitario, FPU-2021) from the Ministerio de Educación, Cultura y Deporte. RF-J is the recipient of grant PI22/01560 funded by the ISCIII and co-funded by the European Union The CNIC is supported by the ISCIII, the Ministerio de Ciencia, Innovación y Universidades (MCIUN) and the Pro CNIC Foundation and is a Severo Ochoa Center of Excellence (grant CEX2020-001041-S funded by MICIN/AEI/10.13039/501100011033).

Running title:
MR-derived strain in adolescents

ABSTRACT

Background

Myocardial strain is a promising marker for the detection of early left or right ventricular (LV or RV) dysfunction in pediatric populations. The reference standard for MR strain measurement is myocardial tagging (MT); however, MT has limited clinical utility because the additional acquisitions needed are time-consuming. In contrast, MR-feature tracking (FT) allows strain quantification from routinely-acquired cine sequences. Studies providing reference values obtained with both FT and MT for adolescents are lacking.

Purpose

To use MR-FT and MT to define sex-specific LV and RV strain reference values for adolescents.

Study type

Cross-sectional, prospective.

Population

123 adolescents aged 15-18 years (52% girls) without known cardiovascular disease.

Field strength/Sequence

Balanced steady-state free-precession sequence for FT analysis and a spatial modulation of magnetization hybrid TFE-EPI sequence for MT acquisitions at 3.0-T.

Assessment

Segment Medviso software was used to obtain longitudinal (LS) and circumferential (CS) strain for both ventricles, and radial strain (RS) for LV.

Statistical tests

The Student t-test was used for between-sex comparisons of continuous variables. Sex-specific percentiles were calculated using the weighted average method. Intraobserver and interobserver agreement was assessed in 30 randomly-selected studies using

intraclass correlation coefficients (ICC). A p-value <0.05 was considered statistically significant.

Results

FT-derived LVLS and LVCS were significantly higher in girls than in boys (-19.8 vs -17.8% and -22.2 vs -21.0%, respectively), as they were with MT (LVLS: -18.1 vs -16.8%; LVCS: -20.8 vs -19.7%). FT-LVRS was higher in girls than in boys (44.8 vs 35.1%), while MT-LVRS was the opposite (18.6 vs 22.7%). FT-RVLS was higher in girls (-23.4 vs -21.3%), but there were no between-sex differences in MT-derived RVLS or RVCS. ICC values for intraobserver agreement were ≥0.89, whereas for interobserver agreement were <0.80 for MT-LVRS and ≥0.80 for all remaining parameters.

Data conclusion

This study provides sex-specific reference biventricular strain values obtained with MR-MT and MR-FT for adolescents aged 15–18 years. MR-FT may be a valid method for obtaining strain values in pediatric populations.

Keywords: Adolescent, Strain, Feature Tracking, Myocardial Tagging.

INTRODUCTION

MRI is an important imaging modality for the evaluation of heart structure and myocardial contractile function in the pediatric population [1]. However, global measures, such as left or right ventricular ejection fraction (LVEF, RVEF), may not be sensitive enough to detect subtle changes in contractile function in individuals with incipient disease [2]. Myocardial strain is defined as the relative change in fiber length from end-diastole, and can be measured in three principal directions (longitudinal, circumferential, and radial) relative to the central ventricular axis [2]. Compared with ejection fraction, global strain values provide a more sensitive measure of myocardial contractile dysfunction in pediatric populations in diverse settings, including muscular dystrophy [3], cancer remission [4], left ventricular non compaction [5], and hypertrophic cardiomyopathy [6].

Cardiac strain can be measured with several MRI techniques [1]. The current reference standard for the assessment of myocardial motion with MRI is myocardial tagging (MT) [7]. However, MT requires specific acquisitions and complex post-processing analysis and is therefore mainly confined to the research environment [2]. A less time-consuming approach to strain measurement is MR feature tracking (FT), which quantifies strain from routinely acquired MR cine images [1].

There is little available information on MR-FT-derived strain values in pediatric populations. The few published studies examined broad age ranges encompassing the whole of childhood and adolescence, with small sample sizes in each age subcategory [8–10]. Furthermore, strain reference values measured with both FT and MT in a pediatric population with no known heart disease are lacking.

Thus, the aim of the this study was to use MR-FT and -MT techniques to establish sex-specific biventricular strain reference values in adolescents aged 15 to 18 years with no known cardiovascular disease.

METHODS

Study population

The study protocol was approved by the research ethics committee of the *Instituto de Salud Carlos III* in Madrid, under identifier CEI PI 63_2020. This study enrolled adolescents aged 15 to 18 years as part of the Early ImaginG Markers of unhealthy lifestyles in Adolescents (EnIGMA) study [11]. For recruitment, the study took advantage of a cluster-randomized trial (NCT03504059) that tested two different health promotion strategies in 1326 adolescents attending 24 public secondary schools in Spain [12]. A detailed analysis of participant cardiovascular health status at enrollment can be found elsewhere [13]. Overall, the tested school-based health promotion strategies had a neutral effect on the cardiovascular health of adolescents at the end of the trial [14]. For inclusion in the EnIGMA study, adolescents needed to be enrolled in the cited trial and to attend one of the 7 schools in the trial located in the Madrid region as of December 2020. The MR scan was performed coincident with the final assessment period of the trial. Exclusion criteria were general contraindications for an MR examination (pacemakers, cochlear implants, known claustrophobia, etc.), pregnancy, and evidence or history of cardiovascular disease. Time spent in moderate-to-vigorous physical activity was estimated with an Actigraph wGT3X-BT accelerometer that the participant wore for 7 consecutive days [15].

All adolescents meeting the inclusion criteria were invited to participate through printed and email invitation letters sent to them and their parents or caregivers. Those who showed interest were invited to virtual meetings in which the study was presented and questions answered by investigators and clinicians leading the study. Invitees who verbally agreed to participate were scheduled to attend the imaging facilities at the *Centro Nacional de Investigaciones Cardiovasculares* (CNIC), where informed consent was

signed and the MR scan performed. Informed consent was signed by the adolescent and at least one parent/caregiver.

MR imaging acquisition protocol

MR examinations were conducted between March 2021 and October 2021 using a Philips 3-T Elition X whole-body scanner (Philips Healthcare, Best, The Netherlands) equipped with a 28-element phased-array Torso-Cardiac coil. Body weight, height, and blood pressure were measured immediately before the MR examination. The imaging protocol did not include administration of intravenous gadolinium contrast.

The protocol included a balanced segmented cine steady-state free-precession (bSSFP) sequence to provide images for the assessment of cardiac chamber dimensions and function. Multi-slice 2D cine MR images were acquired using a bSSFP sequence with the following parameters: temporal resolution 30 ms, field of view (FOV), 380 x 330 mm; voxel size, 1.9 x 1.9 mm; repetition time (TR), 2.7 ms; echo time (TE), 1.35 ms; flip angle, 40°; number of cardiac phases, 30, using retrospective cardiac triggering. A compressed SENSE acquisition factor of 3 was applied in the phase-encoding direction. In addition to 4-chamber (4-Ch) and 2-chamber (2-Ch) long-axis acquisitions, the entire left ventricle (LV) was covered by 9-13 short-axis slices, with a slice thickness of 8 mm and no gap between slices. Participant heart rate was recorded during bSSFP MR acquisition.

MT images were acquired using the spatial modulation of magnetization (SPAMM) tagging technique by means of a hybrid T1 TFE-EPI readout (TFE factor of 3 and EPI factor of 3). Images were acquired with an in-plane spatial resolution of 2.0x2.0 mm^2, a slice thickness of 8mm, and 20 cardiac phases using prospective cardiac triggering, with a tag spacing of 7 mm in both directions, rotated by 45º. Tagging

acquisitions included the long-axis 4-Ch view and three short-axis ventricular slices (basal, mid, and apical; at the mitral-valve, papillary muscle, and apical levels, respectively). Temporal and spatial resolutions to adequately sample ventricular strain were selected following the recommendations given by the Society for Cardiovascular Magnetic Resonance (SCMR) protocols document [16].

MR imaging analysis

A detailed description of biventricular volumetric and functional analysis (including biventricular end-diastolic volumes, LV end-diastolic mass as well as LVEF and RVEF) in this population can be found elsewhere (imaging analysis performed by GP, 14 years of experience; and IG-L, 11 years of experience) [11]. Myocardial strain analysis for tagged and bSSFP images was performed with Segment Medviso software (Lund, Sweden). This software application obtains myocardial strain curves by computing inter-frame deformation fields using a tracking strategy based on non-rigid image registration [17]. For FT short-axis analysis, three slices were selected (basal, mid, and apical) analogous to those acquired with MT, and the long-axis analysis was performed in the 4-Ch and 2-Ch views. MT short-axis analysis was performed in the three short-axis slices acquired (basal, mid, and apical), and the long-axis analysis was performed in the 4-Ch view. Circumferential and radial strain were assessed for both ventricles on short-axis bSSFP and tagged images. Longitudinal strain was assessed on the 4-Ch and 2-Ch views for FT analysis and on the 4-Ch view for MT analysis.

Both LV endocardial and epicardial contours and right ventricle (RV) endocardial contours were drawn in the end-diastolic phase in the short and long axis slices (**Figures 1 and 2**). For the purpose of the analysis, papillary muscles were excluded from the LV myocardial wall in the short and long axis views. Contours were automatically propagated throughout the cardiac cycle. If tracking was suboptimal, the end-diastolic contour was

manually adjusted and re-propagated. If the myocardium was not correctly followed throughout the cardiac cycle, the slice was deleted from the analysis. Strain imaging analysis was performed by CR (4 years of experience). Rotation was defined for each short axis slice as the average angular displacement in the LV wall (degrees). Torsion (also referred to as "normalized twist") [18] was defined as the difference between the rotation in the basal and apical slices normalized by the distance between them as calculated from the sum of inter-slice gaps and slice thicknesses (mm). Strain rate was defined as the time rate of strain change, expressed in inverse seconds ($seconds^{-1}$), both in peak systole and early diastole.

Statistical analysis

Study data were collected and managed using the REDCap electronic data capture tool hosted at the CNIC. Normal distribution assumptions were verified with the use of box plots, normal probability plots, and density function histograms. Continuous variables are presented as mean ± standard deviation (SD), and categorical variables are presented as frequencies and percentages, unless otherwise specified. The Student t-test was used for between-sex comparisons of normally-distributed continuous variables. Multiple linear regression was used to assess adjusted between-sex differences. Sex-specific percentiles were calculated using the weighted average method.

Intraobserver and interobserver agreement was assessed in 30 randomly selected participant studies with intraclass correlation coefficients (ICC) and Bland-Altman plots (Observer 1: CR, 4 years of experience; Observer 2: RP, 3 years of experience). ICC values and their 95% confidence intervals (CI) were calculated using the Stata's *icc* command for two-way random-effects models. Agreement was considered poor, moderate, good, or excellent for ICC <0.50, 0.50 to 0.75, 0.75 to 0.90, and >0.90,

respectively [19]. For Bland-Altman analysis, no significant systematic bias was assumed if the 95% limits of agreement contained the value of 0.

A retrospective power analysis was conducted based on data from the present study (n=123), which compared by-sex differences in strain parameters. Considering a minimum difference to detect of 1.0% in strain values, with a significance criterion of α=0.05, the power of the study was 78.5%. All statistical analyses were performed with Stata software package version 16 (StataCorp, College Station, Texas).

RESULTS

General characteristics

The study-participant flow diagram has been published elsewhere [11]. Of the 124 participants who gave written informed consent, one was unable to undergo the MR examination due to claustrophobia. The analysis thus included 123 participants, with a mean age of 16.0±0.5 years, of whom 52% were girls. Most adolescents (n=117, 95%) were born in Spain, and among these, 26 (22%) had a migrant background (at least one parent/caregiver born outside Spain). Five participants (~4%) were born in Latin America and one (~1%) was born in Africa. Participant characteristics are shown in **Table 1**. Boys had significantly higher weight, height, body surface area, LV mass and biventricular end-diastolic indexed volumes than girls. However, no between-sex significant differences were found in body mass index (p=0.698), LVEF (p=0.412) or RVEF (p=0.085).

Left and right ventricular global strain reference values

For the FT analysis, all cine images could be included. However, 26 slices (7% of all short-axis slices) had to be excluded from the MT analysis due to poor myocardial tracking by the software.

Descriptive summary statistics of the global MR-derived strain values are shown in **Table 2**. LV longitudinal strain (LS) and circumferential strain (CS) were significantly higher in girls than in boys according to both FT and MT techniques [(FT: -19.8±1.7 vs -17.8±2.0 for LS; -22.2±2.7 vs -21.0±2.2 for CS) (MT:-18.1±1.7 vs -16.8±1.7 for LS; and -20.8±2.5 vs -19.7±2.1 for CS)]. However, LV radial strain (RS) was significantly higher in girls as measured by FT (44.8 vs 35.1%) but significantly higher in boys as measured by MT (18.6 vs 22.7%). Regarding RV measurements, RV LS was significantly higher

in girls than in boys as measured by FT (-23.4 vs -21.3%). However, there was no significant difference in RV LS between boys and girls as measured by MT (p=0.514). No between-sex difference was found between boys and girls in RV CS by either FT or MT (p=0.112 and p=0.313, respectively). All significant differences remained statistically significant after adjusting for age and physical activity. Sex-stratified reference values for these global strain values, in the form of user-friendly percentiles, are provided in **Figures 3 and 4**.

Left and right ventricular strain rate reference values

The descriptive summary statistics of the strain rate values, as well as LV torsion, are shown in **Table S1**, and the reference percentiles for these values are provided in **Tables S2 and S3**. LV early diastolic longitudinal and circumferential strain rate (SR) values were significantly higher in girls than in boys, quantified by both FT and MT techniques, as were LV torsion values. LV peak systolic longitudinal SR was significantly higher in girls as measured by FT but not by MT (p=0.060). No between-sex difference was found between boys and girls in LV peak systolic circumferential SR by either FT or MT (p=0.286 and p=0.515, respectively). RV early diastolic SR values were significantly higher in girls than in boys as measured by FT, but not by MT (p=0.479 and p=0.482 for longitudinal and circumferential SR, respectively). Similarly, RV peak systolic longitudinal SR was higher in girls than in boys as measured with FT but not with MT (p=0.167). Finally, there was no significant difference in RV peak systolic circumferential SR between boys and girls as measured by either FT or MT (p=0.783 and p=0.899, respectively).

Reproducibility of the feature-tracking and myocardial tagging techniques

ICCs for intraobserver and interobserver variability are shown in **Tables S4 and S5**, respectively. ICC values for intraobserver reproducibility were ≥0.89 for all LV and RV strain parameters measured. For interobserver reproducibility, ICC values for LV RS as assessed by MT were 0.67 (absolute-agreement) and 0.77 (consistency-of-agreement), and were ≥0.80 for all remaining LV and RV parameters quantified by MT and FT.

Bland-Altman plots for intraobserver and interobserver variability for all strain parameters are shown in **Figures 5 and 6,** respectively. Corresponding bias and upper and lower limits of agreement are shown in **Tables S6 and S7**, respectively. No systematic bias was found for any of the parameters analyzed.

DISCUSSION

This study provides sex-stratified MR-derived strain reference values for adolescents aged 15 to 18 years with no known cardiovascular disease using the FT and MT techniques in a 3-Tesla scanner. MR-FT showed slightly better interobserver reproducibility than MT, the latter considered the reference standard despite being more difficult to implement in daily clinical practice.

According to the recent SCMR consensus document for MRI of pediatric heart disease, MR strain is a promising technique for the detection of early left or right ventricular dysfunction in pediatric populations [1]. The information provided in the current study may thus be useful for clinical practice and may help to detect subtle changes at subclinical disease stages. Furthermore, reference values in young populations may help to bridge the gap in knowledge about the normal physiological changes occurring from childhood to adulthood.

Reference strain values

Our study was performed using a 3-Tesla scanner, and the reference strain values were obtained with Segment Medviso software in an adolescent population with no known cardiovascular disease. The Medviso software program has been reported to have the highest reproducibility of the four main commercial options available [20]. There is very little published information on reference strain values in pediatric populations with no known cardiovascular disease [8–10]. Compared with a study reporting MR-FT-derived reference strain values for children, our study showed numerically higher mean LV LS and RV LS (-18.9% vs -17.5% and -22.4% vs -18.0%, respectively) [9]. MR strain in that study was analyzed with a different software program (TomTec Imaging Systems). The fact that different software programs can provide slightly different strain values reinforces

the importance of comparing and tracking individual values using software from the same vendor [20]. A previous echocardiography study has demonstrated a parabolic evolution of LV strain with age, with low values in infants and in adulthood and peak values coinciding with adolescence [21]. A possible explanation for this could be a physiological adaptation to the increased oxygen demand associated with increasing body mass, and hormonal factors may also be involved [21]. In this regard, the values obtained in our study may shed light on the process of cardiac maturation in adolescence. Also, the variation of strain values with age underlines the need for reference values for each age band. Our study contributes to the literature by focusing on adolescents aged 15 to 18 years an age band in which MR can be performed without sedation, which is likely to encourage its more widespread use.

Differences in strain values by sex

Previous pediatric studies have shown no difference in strain values between boys and girls [8–10]. In contrast, MR-FT studies in adults have reported significantly higher longitudinal strain in females than males, in line with our results [2, 22]. The reason for this difference is unclear. Some authors have related it to hormonal changes during adolescence, including changes in androgens and estrogens, which are known to influence cardiac contractility [10]. Others have proposed that the sex-specific difference in myocardial volumes, which becomes more apparent in adolescence [11], would require greater myocardial shortening in adolescent girls in order to generate a cardiac output similar to that of boys [22]. Another factor could be the higher body surface area (BSA) and height of boys, since afterload increases with height and BSA, and increased afterload is inversely related to strain [23, 24]. Consistent with this, the present study has shown higher values of LV early diastolic strain rate, a marker of diastolic function, in girls.

These results are in agreement with a previous study conducted in adults [25] but not in other studies including younger children [10, 20].

Having strain reference values for the adolescent population is of potential importance. Strain values obtained with MR-MT have been shown to detect early cardiotoxicity in children undergoing anthracycline therapy and with normal indices of global systolic function [4]. Moreover, LV LS values obtained with MR-FT has enabled the detection of subtle LV systolic function abnormalities in a pediatric population with pectus excavatum [26]. In addition, MR-derived strain values can have prognostic value in diseases that appear in childhood and adolescence. For example, MR-FT derived LV strain values have provided independent prognostic value in acute myocarditis, which tends to appear in early adolescence or young adulthood [27], and a retrospective MR-FT study has shown an association between decreased LV RS and LV LS values and adverse outcomes in a pediatric population with hypertrophic cardiomyopathy [6]. RV strain, though less studied than LV strain, has shown prognostic value for the incidence of ventricular arrhythmias in a population with arrhythmogenic right ventricular cardiomyopathy [28].

Reproducibility of MR strain techniques

MR has been an established modality for measuring myocardial strain since the first description of MT in 1988 [29]. The SPAMM technique— currently the most widely used technique for MT—creates a grid of radiofrequency tags that moves with the myocardium, enabling tracking of cardiac deformation. MT has been extensively validated and has thus served as the reference standard for validation of other strain techniques, including speckle-tracking echocardiography [30]. However, the need to acquire additional images and complex post-processing has limited the use of MR-MT in clinical practice [31]. In comparison, MR-FT is easier to perform and avoids the need for

additional acquisitions and complex post-processing because it uses routinely acquired cine images. MR-FT is based on a block-matching approach, identifying anatomic features in MR images (a myocardial band defined by the endocardial border) and tracking them over the cardiac cycle by searching for the most comparable image pattern in the next image [32].

In a previous adult study, FT gave higher estimates of LV LS and RS than MT, whereas FT- and MT-derived LV CS values were in reasonable agreement [33]. However, FT has shown excellent reproducibility [34]. The present study compared the reproducibility of these techniques in adolescents with no known cardiovascular disease. Consistent with previous reports [33, 35], FT gave a slightly higher estimate of LV longitudinal and circumferential strain than MT, but the FT estimate was more reproducible with the commercial software used in the present study. Similarly, in agreement with a prior report [33], our study showed that the estimates of LV radial strain by FT almost doubled the values obtained with MT, being also the least reproducible parameter. The different values obtained by FT and MT may be at least partly explained because of technical reasons. Changes in the voxel pattern during the cardiac cycle within the myocardium may have an impact on consistency of FT and account for some variation in strain measures, particularly in the radial direction [33]. Furthermore, a previous study has shown that strain values have a transmural gradient, being higher in the endocardial layer [35]. The fact that FT tracks deformation predominantly at the endocardial level could contribute explaining the higher values derived from this technique as compared to MT. As a consequence, radial strain values in particular should be interpreted with caution, especially if derived from different imaging techniques and/or software.

Given that children find it more difficult than adults to remain still inside a scanner for long periods, studies of pediatric populations would likely benefit from a reduction in

MR acquisition times, achieved either by limiting the acquisition of tagged images or by the use of ultrafast imaging protocols [36]. The reference values provided in this study may be clinically useful because myocardial strain can be altered in the initial stages of heart disease, before the appearance of classical disease indicators, and altered strain values have shown prognostic value in cardiac diseases affecting adolescents [4, 6, 26, 37].

Limitations

This study reports MR-derived strain reference values obtained in a relatively large adolescent sample in Spain. The geographical restriction of the sample could limit the applicability of these reference values in other locations. Also, the results obtained with the specific software application used here might be incompatible with those obtained with applications from a different vendor, and it therefore advisable to use the same software package for longitudinal or clinical follow-up of the same individual. Although several other quantitative techniques have been proposed to measure strain such as displacement encoding with stimulated echoes (DENSE), strain encoding (SENC) or tissue velocity mapping, these methods require additional acquisitions and time. We did not consider performing any of these additional sequences in the MR protocol in order to limit scanner acquisition time in the pediatric population included in the study. The same reason precluded the acquisition of serial repeated scans and therefore, inter-study reproducibility could not be assessed. Finally, long axis 2-chamber views were not obtained for MT analysis and 3-chamber views were not obtained for any technique, which could limit the reproducibility of strain values obtained. However, the absence of cardiovascular disease in the study participants makes regional differences in strain values unlikely.

Conclusions

This study provides sex-stratified MR-derived biventricular strain reference values obtained with two methods, FT and MT, in an adolescent population with no known cardiovascular disease. The FT technique does not require additional image acquisition and showed good agreement and reproducibility. Therefore, it may be a valid technique for obtaining biventricular MR-derived strain values in pediatric populations.

REFERENCES

1. Dorfman AL, Geva T, Samyn MM, et al (2022) SCMR expert consensus statement for cardiovascular magnetic resonance of acquired and non-structural pediatric heart disease. J Cardiovasc Magn Reson 24:44. https://doi.org/10.1186/s12968-022-00873-1

2. Taylor RJ, Moody WE, Umar F, et al (2015) Myocardial strain measurement with feature-tracking cardiovascular magnetic resonance: normal values. Eur Hear J – Cardiovasc Imaging 16:871–881. https://doi.org/10.1093/ehjci/jev006

3. Ashford MW, Liu W, Lin SJ, et al (2005) Occult Cardiac Contractile Dysfunction in Dystrophin-Deficient Children Revealed by Cardiac Magnetic Resonance Strain Imaging. Circulation 112:2462–2467. https://doi.org/10.1161/CIRCULATIONAHA.104.516716

4. Toro-Salazar OH, Gillan E, O'Loughlin MT, et al (2013) Occult Cardiotoxicity in Childhood Cancer Survivors Exposed to Anthracycline Therapy. Circ Cardiovasc Imaging 6:873–880. https://doi.org/10.1161/CIRCIMAGING.113.000798

5. Nucifora G, Sree Raman K, Muser D, et al (2017) Cardiac magnetic resonance evaluation of left ventricular functional, morphological, and structural features in children and adolescents vs. young adults with isolated left ventricular non-compaction. Int J Cardiol 246:68–73. https://doi.org/10.1016/j.ijcard.2017.05.100

6. Smith BM, Dorfman AL, Yu S, et al (2014) Relation of Strain by Feature Tracking and Clinical Outcome in Children, Adolescents, and Young Adults With Hypertrophic Cardiomyopathy. Am J Cardiol 114:1275–1280. https://doi.org/10.1016/j.amjcard.2014.07.051

7. Kawel-Boehm N, Hetzel SJ, Ambale-Venkatesh B, et al (2020) Reference ranges ("normal values") for cardiovascular magnetic resonance (CMR) in adults and children: 2020 update. J Cardiovasc Magn Reson 22:87. https://doi.org/10.1186/s12968-020-00683-3

8. Voges I, Negwer I, Caliebe A, et al (2022) Myocardial Deformation in the Pediatric Age Group: Normal Values for Strain and Strain Rate Using <scp>2D</scp> Magnetic Resonance Feature Tracking. J Magn Reson Imaging 56:1382–1392. https://doi.org/10.1002/jmri.28073

9. Shang Q, Patel S, Steinmetz M, et al (2018) Myocardial deformation assessed by longitudinal strain: Chamber specific normative data for CMR-feature tracking from the German competence network for congenital heart defects. Eur Radiol 28:1257–1266. https://doi.org/10.1007/s00330-017-5034-2

10. André F, Robbers-Visser D, Helling-Bakki A, et al (2017) Quantification of myocardial deformation in children by cardiovascular magnetic resonance feature tracking: determination of reference values for left ventricular strain and strain rate. J Cardiovasc Magn Reson 19:8. https://doi.org/10.1186/s12968-016-0310-x

11. Real C, Párraga R, Pizarro G, et al (2023) Magnetic resonance imaging reference values for cardiac morphology, function and tissue composition in adolescents. eClinicalMedicine 57:101885. https://doi.org/10.1016/j.eclinm.2023.101885

12. Fernandez-Jimenez R, Santos-Beneit G, Tresserra-Rimbau A, et al (2019) Rationale and design of the school-based SI! Program to face obesity and promote health among Spanish adolescents: A cluster-randomized controlled trial. Am Heart J 215:27–40. https://doi.org/10.1016/j.ahj.2019.03.014

13. Fernandez-Jimenez R, Santos-Beneit G, de Cos-Gandoy A, et al (2022) Prevalence and correlates of cardiovascular health among early adolescents enrolled in the SI! Program in Spain: a cross-sectional analysis. Eur J Prev Cardiol 29:e7–e10. https://doi.org/10.1093/eurjpc/zwaa096

14. Santos-Beneit G, Fernández-Alvira JM, Tresserra-Rimbau A, et al (2023) School-Based Cardiovascular Health Promotion in Adolescents. JAMA Cardiol 8:816. https://doi.org/10.1001/jamacardio.2023.2231

15. Martínez-Gómez J, Fernández-Alvira JM, de Cos-Gandoy A, et al (2023) Sleep duration and its association with adiposity markers in adolescence: a cross-sectional and longitudinal study. Eur J Prev Cardiol 30:1236–1244. https://doi.org/10.1093/eurjpc/zwad137

16. Kramer CM, Barkhausen J, Bucciarelli-Ducci C, et al (2020) Standardized cardiovascular magnetic resonance imaging (CMR) protocols: 2020 update. J Cardiovasc Magn Reson 22:17. https://doi.org/10.1186/s12968-020-00607-1

17. Morais P, Marchi A, Bogaert JA, et al (2017) Cardiovascular magnetic resonance myocardial feature tracking using a non-rigid, elastic image registration algorithm: assessment of variability in a real-life clinical setting. J Cardiovasc Magn Reson 19:24. https://doi.org/10.1186/s12968-017-0333-y

18. Kowallick JT, Morton G, Lamata P, et al (2016) Inter-study reproducibility of left ventricular torsion and torsion rate quantification using MR myocardial feature tracking. J Magn Reson Imaging 43:128–137. https://doi.org/10.1002/jmri.24979

19. Koo TK, Li MY (2016) A Guideline of Selecting and Reporting Intraclass Correlation Coefficients for Reliability Research. J Chiropr Med 15:155–163. https://doi.org/10.1016/j.jcm.2016.02.012

20. Barreiro-Pérez M, Curione D, Symons R, et al (2018) Left ventricular global myocardial strain assessment comparing the reproducibility of four commercially available CMR-feature tracking algorithms. Eur Radiol 28:5137–5147. https://doi.org/10.1007/s00330-018-5538-4

21. Marcus KA, Mavinkurve-Groothuis AMC, Barends M, et al (2011) Reference Values for Myocardial Two-Dimensional Strain Echocardiography in a Healthy Pediatric and Young Adult Cohort. J Am Soc Echocardiogr 24:625–636. https://doi.org/10.1016/j.echo.2011.01.021

22. Mangion K, Burke NMM, McComb C, et al (2019) Feature-tracking myocardial strain in healthy adults- a magnetic resonance study at 3.0 tesla. Sci Rep 9:3239. https://doi.org/10.1038/s41598-019-39807-w

23. Chirinos JA, Segers P (2010) Noninvasive Evaluation of Left Ventricular Afterload. Hypertension 56:563–570. https://doi.org/10.1161/HYPERTENSIONAHA.110.157339

24. Donal E, Bergerot C, Thibault H, et al (2009) Influence of afterload on left ventricular radial and longitudinal systolic functions: a two-dimensional strain imaging study. Eur J Echocardiogr 10:914–921. https://doi.org/10.1093/ejechocard/jep095

25. Andre F, Steen H, Matheis P, et al (2015) Age- and gender-related normal left ventricular deformation assessed by cardiovascular magnetic resonance feature tracking. J Cardiovasc Magn Reson 17:25. https://doi.org/10.1186/s12968-015-0123-3

26. Rodriguez-Granillo GA, Toselli L, Farina J, et al (2022) Usefulness of strain cardiac magnetic resonance for the exposure of mild left ventricular systolic abnormalities in pectus excavatum. J Pediatr Surg 57:319–324. https://doi.org/10.1016/j.jpedsurg.2021.09.008

27. Vos JL, Raafs AG, van der Velde N, et al (2022) Comprehensive Cardiovascular Magnetic Resonance-Derived Myocardial Strain Analysis Provides Independent Prognostic Value in Acute Myocarditis. J Am Heart Assoc 11:. https://doi.org/10.1161/JAHA.121.025106

28. Bourfiss M, Prakken NHJ, James CA, et al (2022) Prognostic value of strain by feature-tracking cardiac magnetic resonance in arrhythmogenic right ventricular cardiomyopathy. Eur Hear J - Cardiovasc Imaging 24:98–107. https://doi.org/10.1093/ehjci/jeac030

29. Zerhouni EA, Parish DM, Rogers WJ, et al (1988) Human heart: tagging with MR imaging--a method for noninvasive assessment of myocardial motion. Radiology 169:59–63. https://doi.org/10.1148/radiology.169.1.3420283

30. Salerno M (2018) Feature Tracking by CMR. JACC Cardiovasc Imaging 11:206–208. https://doi.org/10.1016/j.jcmg.2017.01.024

31. Voigt J-U, Cvijic M (2019) 2- and 3-Dimensional Myocardial Strain in Cardiac Health and Disease. JACC Cardiovasc Imaging 12:1849–1863. https://doi.org/10.1016/j.jcmg.2019.01.044

32. Claus P, Omar AMS, Pedrizzetti G, et al (2015) Tissue Tracking Technology for Assessing Cardiac Mechanics. JACC Cardiovasc Imaging 8:1444–1460. https://doi.org/10.1016/j.jcmg.2015.11.001

33. Augustine D, Lewandowski AJ, Lazdam M, et al (2013) Global and regional left ventricular myocardial deformation measures by magnetic resonance feature tracking in healthy volunteers: comparison with tagging and relevance of gender. J Cardiovasc Magn Reson 15:8. https://doi.org/10.1186/1532-429X-15-8

34. Xu J, Yang W, Zhao S, Lu M (2022) State-of-the-art myocardial strain by CMR feature tracking: clinical applications and future perspectives. Eur Radiol 32:5424–5435. https://doi.org/10.1007/s00330-022-08629-2

35. Moody WE, Taylor RJ, Edwards NC, et al (2015) Comparison of magnetic resonance feature tracking for systolic and diastolic strain and strain rate calculation with spatial modulation of magnetization imaging analysis. J Magn Reson Imaging 41:1000–1012. https://doi.org/10.1002/jmri.24623

36. Gómez-Talavera S, Fernandez-Jimenez R, Fuster V, et al (2021) Clinical

Validation of a 3-Dimensional Ultrafast Cardiac Magnetic Resonance Protocol Including Single Breath-Hold 3-Dimensional Sequences. JACC Cardiovasc Imaging 14:1742–1754. https://doi.org/10.1016/j.jcmg.2021.02.031

37. Chungsomprasong P, Hamilton R, Luining W, et al (2017) Left Ventricular Function in Children and Adolescents With Arrhythmogenic Right Ventricular Cardiomyopathy. Am J Cardiol 119:778–784. https://doi.org/10.1016/j.amjcard.2016.11.020

TABLES

Table 1. **Participant characteristics, overall and stratified by sex**

	Total	**Boys**	**Girls**	**p-value**
	N=123	**N=59 (48.0%)**	**N=64 (52.0%)**	
Age, years	16.0 (0.4)	16.1 (0.5)	16.0 (0.4)	0.384
Weight, kg	61.0 (10.5)	65.1 (10.1)	57.2 (9.4)	**<0.001**
Height, m	1.69 (0.09)	1.75 (0.07)	1.63 (0.06)	**<0.001**
BMI, kg/m^2	21.4 (3.2)	21.3 (2.9)	21.5 (3.5)	0.698
BMI z-score	0.09 (0.89)	0.04 (0.97)	0.13 (0.82)	0.586
Body surface area, m^2	1.69 (0.16)	1.79 (0.15)	1.61 (0.12)	**<0.001**
Heart rate, bpm	68.9 (11.0)	68.4 (11.3)	69.3 (10.8)	0.663
Mean blood pressure, mmHg	89.5 (7.6)	90.2 (6.4)	88.8 (8.6)	0.333
iLeft ventricular end-diastolic mass, g/m^2	42.3 (9.9)	48.5 (9.6)	36.6 (6.0)	**<0.001**
iLeft ventricular end-diastolic volume, ml/m^2	84.6 (12.1)	91.7 (11.6)	78.1 (8.3)	**<0.001**
iRight ventricular end-diastolic volume, ml/m^2	92.4 (15.0)	101.3 (14.1)	84.1 (10.5)	**<0.001**
Left ventricular ejection fraction, %	62.5 (4.1)	62.2 (4.1)	62.8 (4.2)	0.412
Right ventricular ejection fraction, %	56.2 (4.6)	55.4 (4.7)	56.8 (4.4)	0.085

Data are presented as mean (SD). P-values denote the significance of between-sex differences for continuous variables analyzed by Student's t-tests. BMI z-scores were defined according to age- and sex-adjusted body mass index percentiles (P) based on Centers for Disease Control reference values. BMI, body mass index. Some of the data presented in this table have been published previously [12].

Table 2. MR-derived strain summarized values, overall and stratified by sex.

	Total	**Boys**	**Girls**	**p-value**
	N=123	**N=59**	**N=64**	
Feature tracking				
LV LS, %	-18.9 (2.1)	-17.8 (2.0)	-19.8 (1.7)	**<0.001**
LV CS, %	-21.6 (2.5)	-21.0 (2.2)	-22.2 (2.7)	**0.007**
LV RS, %	40.2 (10.7)	35.1 (8.1)	44.8 (10.7)	**<0.001**
RV LS, %	-22.4 (3.2)	-21.3 (3.2)	-23.4 (2.9)	**<0.001**
RV CS, %	-13.9 (3.1)	-13.5 (2.9)	-14.3 (3.2)	0.112
Myocardial tagging				
LV LS, %	-17.5 (1.8)	-16.8 (1.7)	-18.1 (1.7)	**<0.001**
LV CS, %	-20.2 (2.4)	-19.7 (2.1)	-20.8 (2.5)	**0.013**
LV RS, %	20.6 (6.1)	22.7 (5.3)	18.6 (6.1)	**<0.001**
RV LS, %	-21.4 (2.8)	-21.2 (2.6)	-21.6 (3.0)	0.514
RV CS, %	-14.5 (2.3)	-14.3 (2.5)	-14.7 (2.0)	0.313

Data are presented as mean (SD). p-values are derived from the analysis of between-sex differences by Student's t-tests. CS, circumferential strain; LS, longitudinal strain; LV, left ventricular; RS, radial strain; RV, right ventricular.

FIGURE TITLES AND LEGENDS

Figure 1. Strain analysis by MR feature tracking.

Representative bSSFP images showing the end-diastolic and end-systolic phases in a study participant: (A) 2-chamber view, (B) 4-chamber view, and (C) short axis mid-ventricular slice. Myocardial contours were drawn in the end-diastolic phase (left column) and they were automatically propagated throughout the cardiac cycle. Derived strain curves are shown to the right: longitudinal strain is obtained from the 2-chamber (A) and 4-chamber (B) views, whereas radial and circumferential strain are obtained from the short-axis slices (C).

Figure 2. Strain analysis by MR myocardial tagging.

Representative SPAMM tagged images showing the end-diastolic and end-systolic phases in a study participant: (A) 4-chamber view, (B) short-axis mid-ventricular slice. Myocardial contours were drawn in the end-diastolic phase (left column) and they were automatically propagated throughout the cardiac cycle. Derived strain curves are shown to the right: longitudinal strain is obtained from the 4-chamber view (A), whereas radial and circumferential strain are obtained from the short-axis slices (B).

Figure 3. MR-derived left ventricular strain reference percentiles in adolescents.

The bars are colored yellow for values between 3rd and 10th percentile and red for values below the 3rd percentile, indicating potentially abnormal values. A: Longitudinal Strain, B: Circumferential Strain, C: Radial Strain. P, percentile.

Figure 4. MR-derived right ventricular strain reference percentiles in adolescents.

The bars are colored yellow for values between 3rd and 10th percentile and red for values below the 3rd percentile, indicating potentially abnormal values. A: Longitudinal Strain, B: Circumferential Strain. P, percentile**.**

Figure 5. Intraobserver reproducibility assessment for strain parameters obtained with feature tracking and myocardial tagging.

Intraobserver reproducibility was assessed with Bland-Altman plots for comparison between the first analysis (Obs1) and second analysis (Obs1bis) performed by observer 1. CS, circumferential strain; LS, longitudinal strain; LV, left ventricular; RS, radial strain; RV, right ventricular.

Figure 6. Interobserver reproducibility assessment for strain parameters obtained with feature tracking and myocardial tagging.

Interobserver reproducibility was assessed with Bland-Altman plots for comparison between analyses performed by Obs1 and observer 2 (Obs2). CS, circumferential strain; LS, longitudinal strain; LV, left ventricular; RS, radial strain; RV, right ventricular.

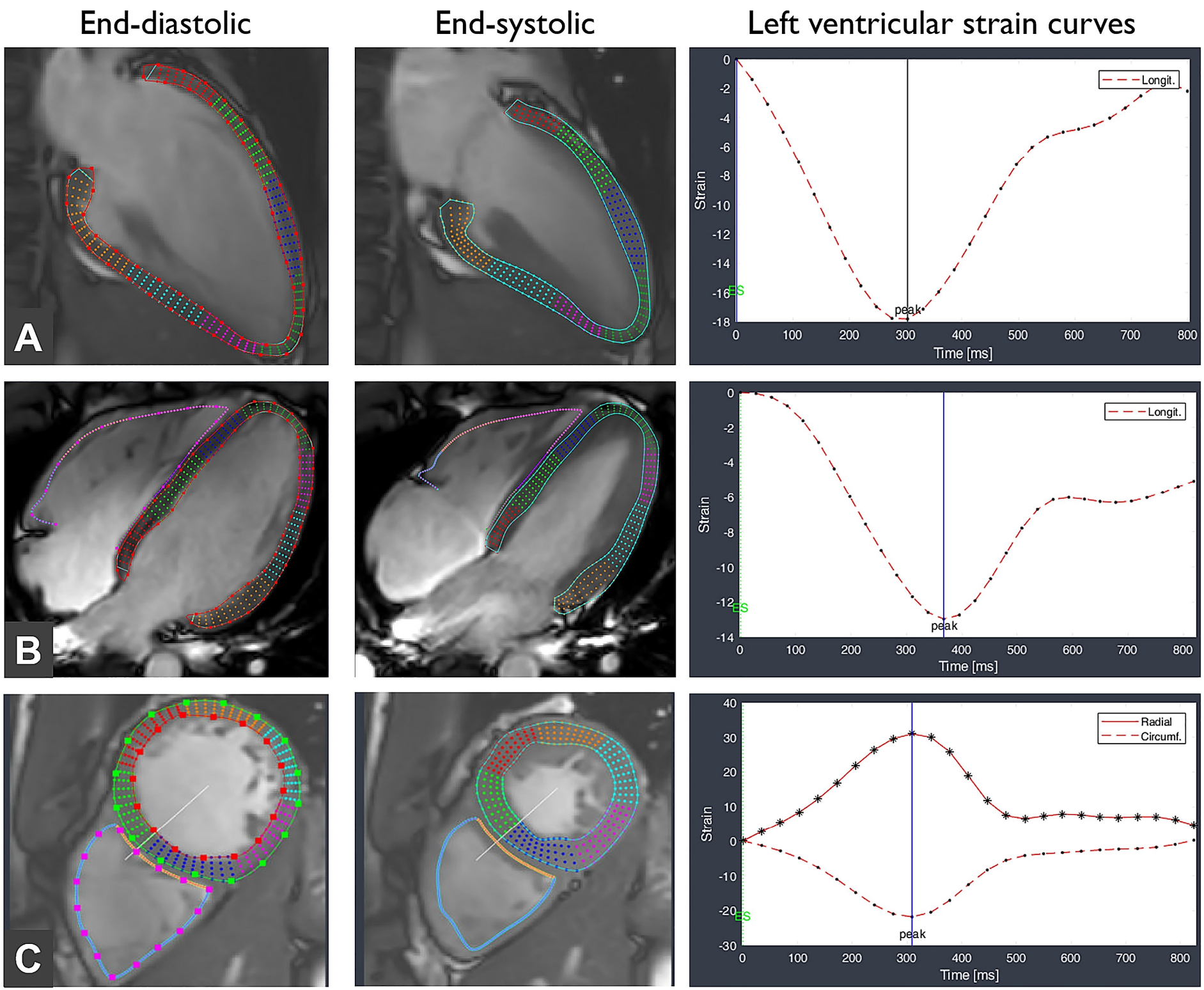
End-diastolic
End-systolic
Left ventricular strain curves
A
B
C
Longit.
Strain
Time [ms]
ES
peak
Radial
Circumf.

End-diastolic

End-systolic

Left ventricular strain curves

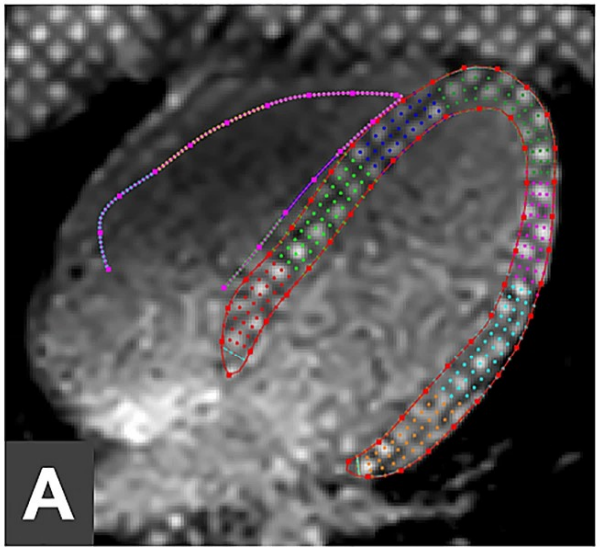

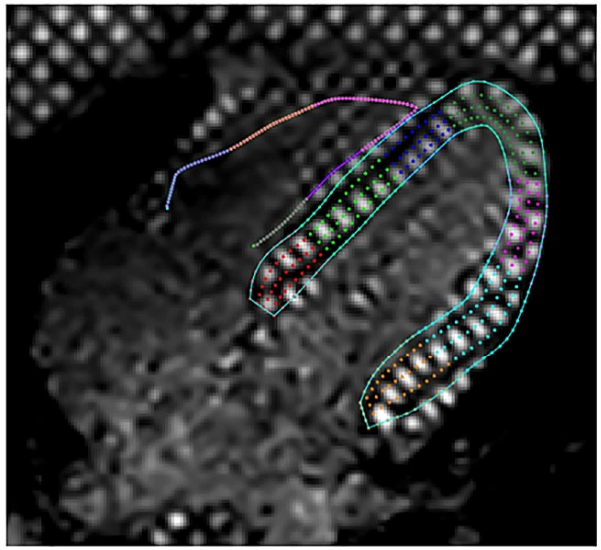

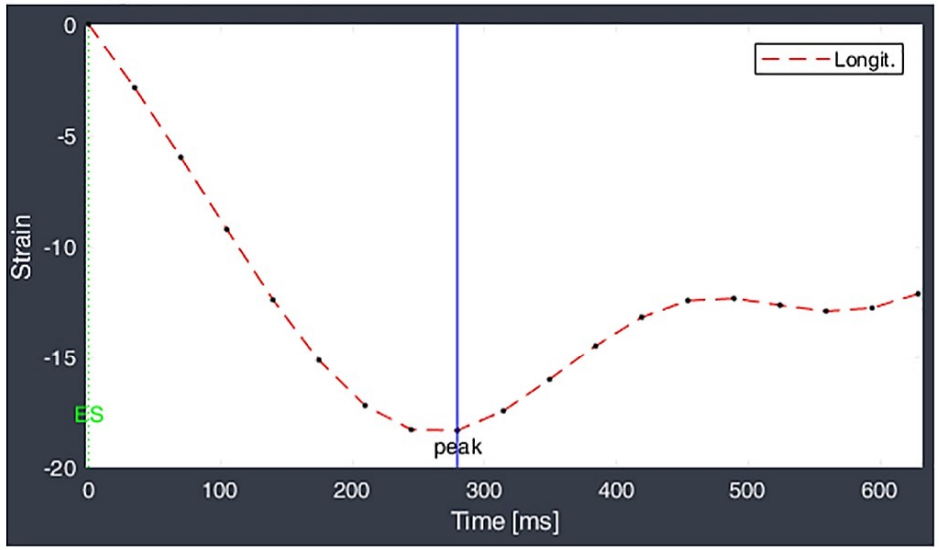

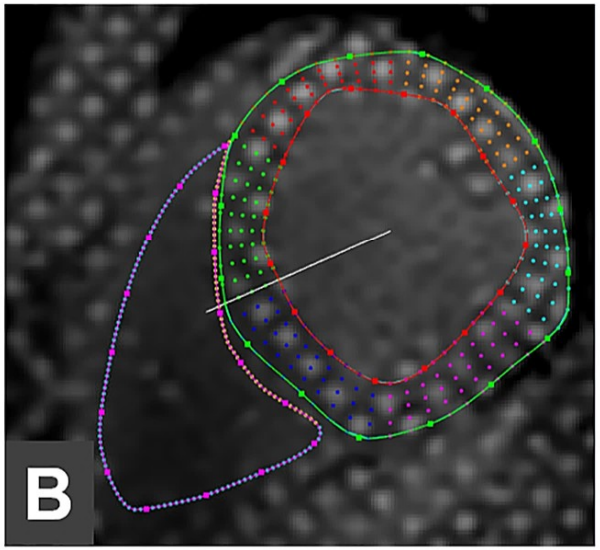

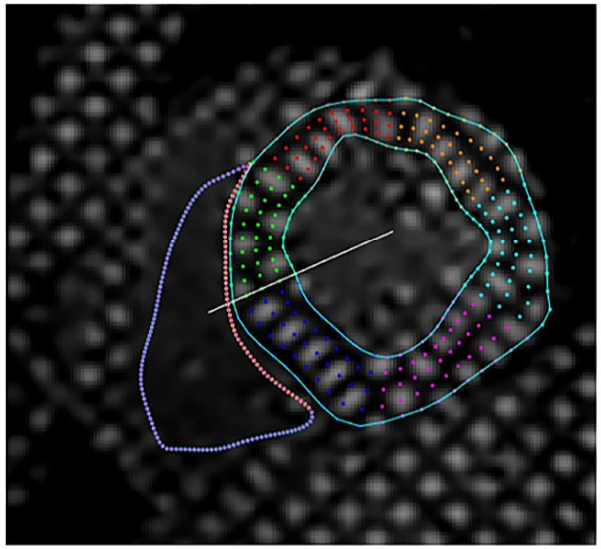

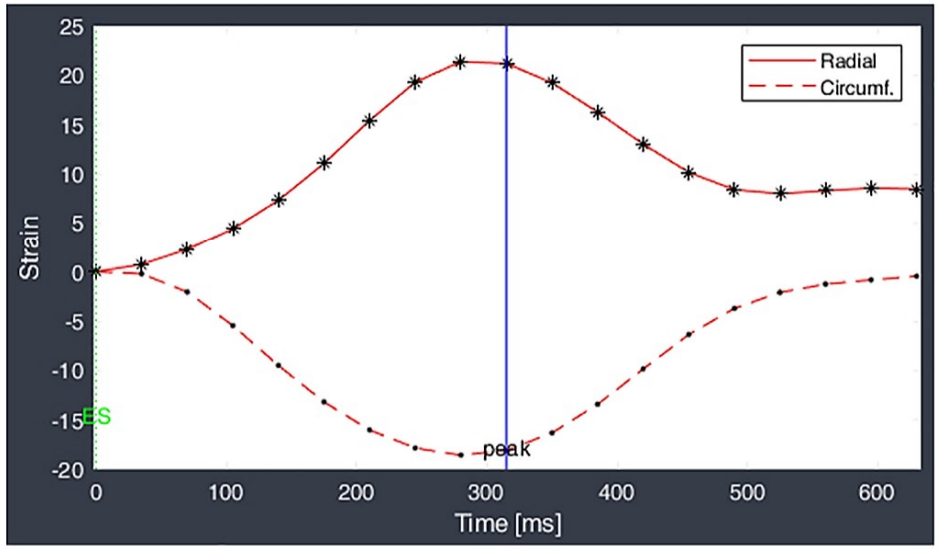

Left Ventricle

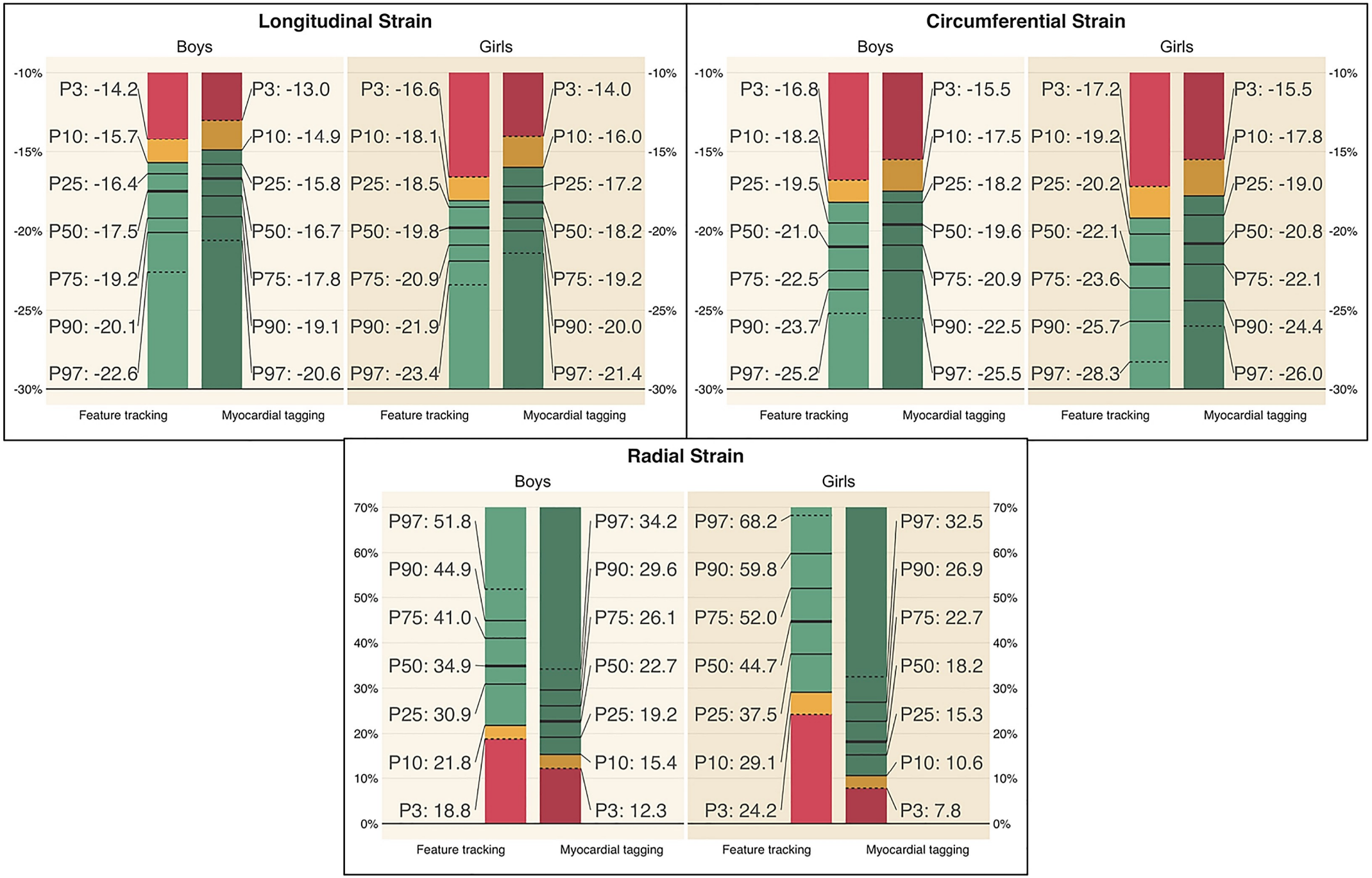

Right Ventricle

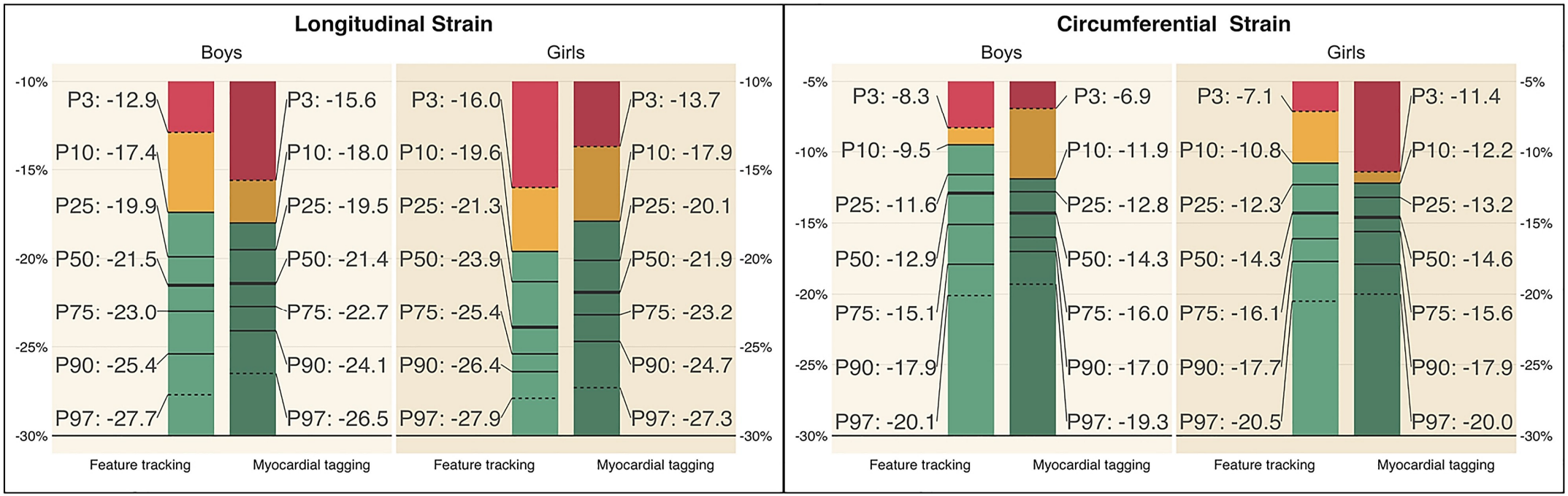

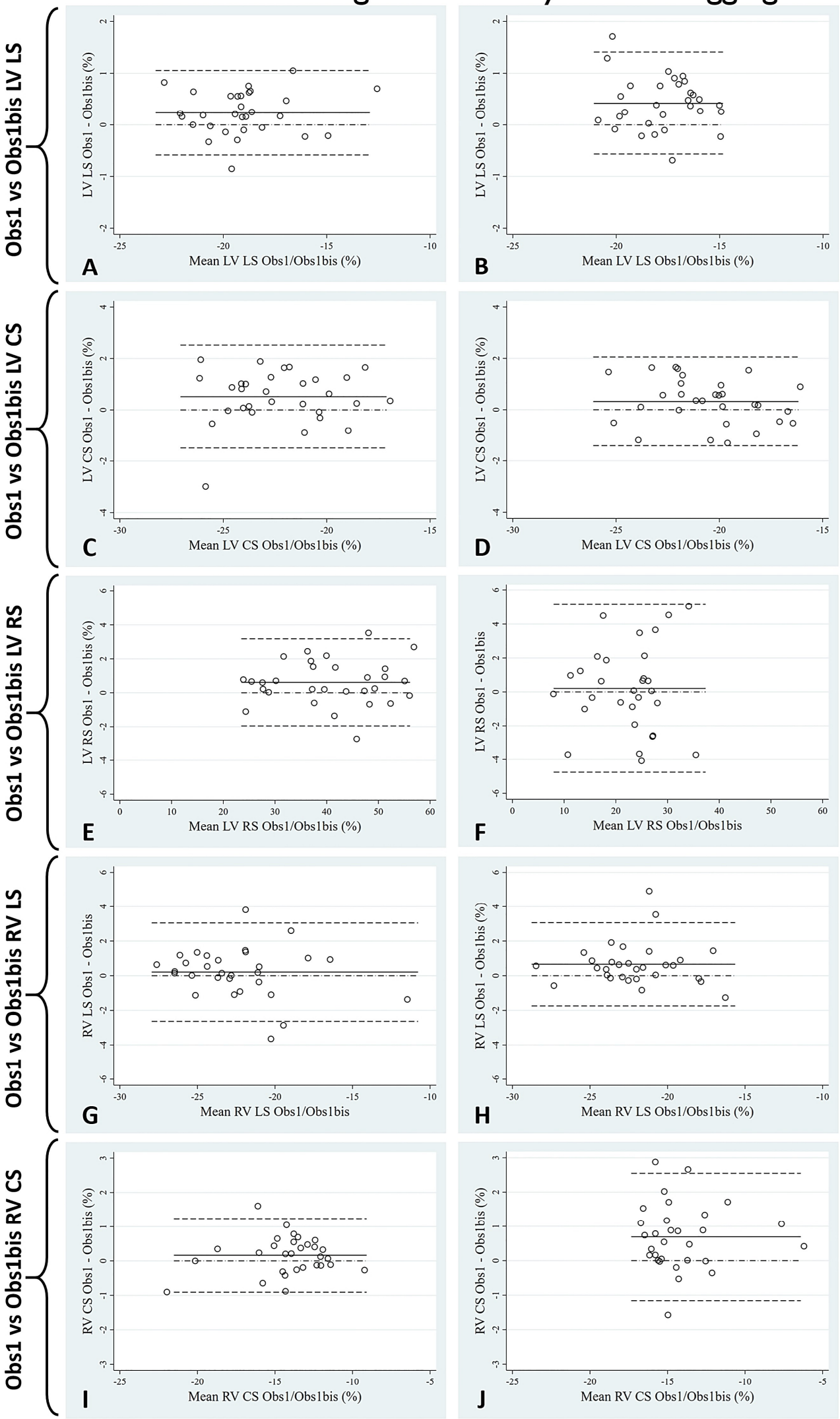
Feature tracking
Myocardial tagging
Obs1 vs Obs1bis LV LS
Obs1 vs Obs1bis LV CS
Obs1 vs Obs1bis LV RS
Obs1 vs Obs1bis RV LS
Obs1 vs Obs1bis RV CS
LV LS Obs1 - Obs1bis (%)
Mean LV LS Obs1/Obs1bis (%)
A
B
LV CS Obs1 - Obs1bis (%)
Mean LV CS Obs1/Obs1bis (%)
C
D
LV RS Obs1 - Obs1bis (%)
LV RS Obs1 - Obs1bis
Mean LV RS Obs1/Obs1bis (%)
Mean LV RS Obs1/Obs1bis
E
F
RV LS Obs1 - Obs1bis
RV LS Obs1 - Obs1bis (%)
Mean RV LS Obs1/Obs1bis
Mean RV LS Obs1/Obs1bis (%)
G
H
RV CS Obs1 - Obs1bis (%)
Mean RV CS Obs1/Obs1bis (%)
I
J

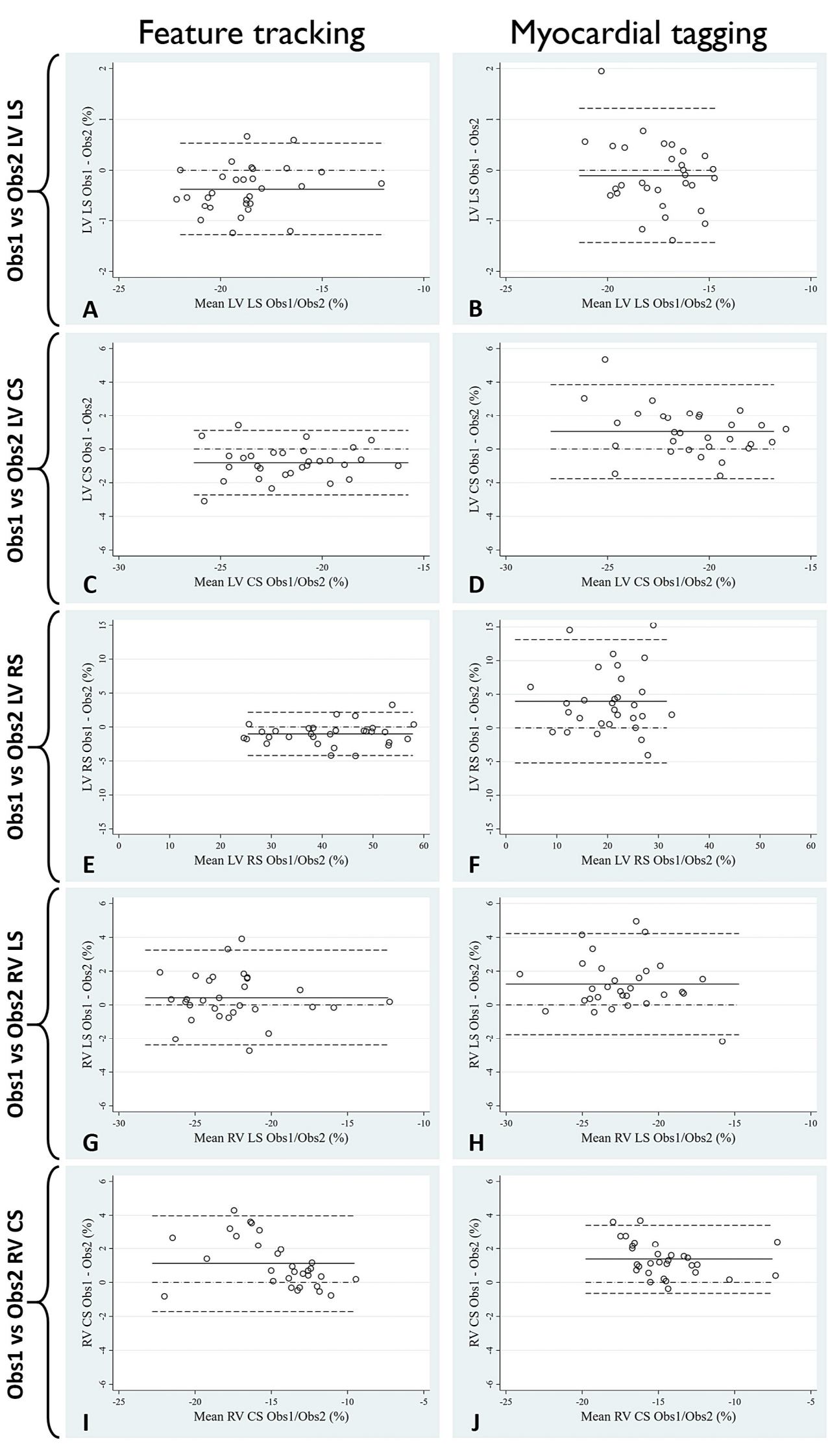
Feature tracking
Myocardial tagging
Obs1 vs Obs2 LV LS
Obs1 vs Obs2 LV CS
Obs1 vs Obs2 LV RS
Obs1 vs Obs2 RV LS
Obs1 vs Obs2 RV CS
LV LS Obs1 - Obs2 (%)
Mean LV LS Obs1/Obs2 (%)
A
LV LS Obs1 - Obs2
Mean LV LS Obs1/Obs2 (%)
B
LV CS Obs1 - Obs2
Mean LV CS Obs1/Obs2 (%)
C
LV CS Obs1 - Obs2 (%)
Mean LV CS Obs1/Obs2 (%)
D
LV RS Obs1 - Obs2 (%)
Mean LV RS Obs1/Obs2 (%)
E
LV RS Obs1 - Obs2 (%)
Mean LV RS Obs1/Obs2 (%)
F
RV LS Obs1 - Obs2 (%)
Mean RV LS Obs1/Obs2 (%)
G
RV LS Obs1 - Obs2 (%)
Mean RV LS Obs1/Obs2 (%)
H
RV CS Obs1 - Obs2 (%)
Mean RV CS Obs1/Obs2 (%)
I
RV CS Obs1 - Obs2 (%)
Mean RV CS Obs1/Obs2 (%)
J

SUPPLEMENTARY MATERIAL

Table S1. Cardiovascular magnetic resonance-derived strain rate summarized values, overall and stratified by sex

	Total	**Boys**	**Girls**	**p-value**
	N=123	**N=59**	**N=64**	
Feature tracking				
LV LDSR, 1/s	0.81 (0.22)	0.73 (0.21)	0.88 (0.21)	**<0.001**
LV LSSR, 1/s	-0.82 (0.12)	-0.79 (0.12)	-0.86 (0.10)	**0.001**
LV CDSR, 1/s	1.21 (0.28)	1.14 (0.24)	1.28 (0.30)	**0.006**
LV CSSR, 1/s	-1.11 (0.20)	-1.09 (0.19)	-1.13 (0.20)	0.286
LV RDSR, 1/s	-2.60 (0.87)	-2.20 (0.60)	-2.96 (0.93)	**<0.001**
LV RSSR, 1/s	1.68 (0.47)	1.52 (0.36)	1.83 (0.51)	**<0.001**
RV LDSR, 1/s	0.89 (0.25)	0.82 (0.22)	0.95 (0.26)	**0.003**
RV LSSR, 1/s	-0.98 (0.17)	-0.93 (0.17)	-1.01 (0.15)	**0.009**
RV CDSR, 1/s	0.70 (0.20)	0.63 (0.17)	0.77 (0.20)	**<0.001**
RV CSSR, 1/s	-0.61 (0.16)	-0.61 (0.14)	-0.62 (0.17)	0.783
Myocardial tagging				
LV LDSR, 1/s	0.65 (0.20)	0.60 (0.19)	0.69 (0.20)	**0.008**
LV LSSR, 1/s	-0.85 (0.10)	-0.83 (0.09)	-0.86 (0.10)	0.060
LV CDSR, 1/s	1.11 (0.17)	1.08 (0.16)	1.14 (0.18)	**0.031**
LV CSSR, 1/s	-1.05 (0.12)	-1.04 (0.12)	-1.06 (0.13)	0.515
LV RDSR, 1/s	-0.93 (0.36)	-1.03 (0.41)	-0.84 (0.27)	**0.002**
LV RSSR, 1/s	1.24 (0.27)	1.31 (0.25)	1.18 (0.27)	**0.004**
LV Torsion, degrees/mm	0.23 (0.07)	0.21 (0.06)	0.24 (0.08)	**0.007**
RV LDSR, 1/s	0.93 (0.26)	0.95 (0.22)	0.91 (0.29)	0.479
RV LSSR, 1/s	-0.94 (0.13)	-0.95 (0.14)	-0.92 (0.13)	0.167
RV CDSR, 1/s	0.74 (0.18)	0.75 (0.16)	0.73 (0.19)	0.482
RV CSSR, 1/s	-0.72 (0.13)	-0.71 (0.13)	-0.72 (0.13)	0.899

Data are presented as mean (SD). P-values are derived from the analysis of between-sex differences by the Student t-test. CDSR, circumferential early diastolic strain rate; CSSR, circumferential peak systolic strain rate; LDSR, longitudinal early diastolic strain rate; LSSR, longitudinal peak systolic strain rate; LV, left ventricle; RDSR, radial early diastolic strain rate; RSSR, radial peak systolic strain rate, RV, right ventricle

Table S2. Cardiovascular magnetic resonance feature tracking-derived strain rate reference percentiles in adolescents.

	BOYS							GIRLS						
	Percentiles							Percentiles						
	3	10	25	50	75	90	97	3	10	25	50	75	90	97
Feature tracking														
LV LDSR, 1/s	0.41	0.50	0.56	0.73	0.90	0.98	1.22	0.50	0.61	0.72	0.87	1.02	1.18	1.28
LV LSSR, 1/s	-0.58	-0.63	-0.70	-0.77	-0.87	-0.97	-1.04	-0.65	-0.72	-0.79	-0.85	-0.93	-0.99	-1.07
LV CDSR, 1/s	0.74	0.86	0.96	1.11	1.30	1.44	1.66	0.82	0.96	1.05	1.23	1.44	1.68	1.92
LV CSSR, 1/s	-0.81	-0.86	-0.94	-1.08	-1.24	-1.34	-1.57	-0.83	-0.89	-1.00	-1.09	-1.26	-1.41	-1.68
LV RDSR, 1/s	-1.22	-1.44	-1.67	-2.21	-2.77	-3.04	-3.38	-1.51	-1.92	-2.28	-2.90	-3.49	-4.29	-5.02
LV RSSR, 1/s	0.77	1.04	1.31	1.47	1.85	2.03	2.19	0.89	1.19	1.47	1.82	2.13	2.52	2.94
RV LDSR, 1/s	0.44	0.54	0.66	0.82	1.00	1.10	1.27	0.37	0.58	0.80	0.95	1.14	1.27	1.52
RV LSSR, 1/s	-0.58	-0.71	-0.80	-0.94	-1.07	-1.18	-1.24	-0.62	-0.82	-0.90	-1.03	-1.11	-1.21	-1.32
RV CDSR, 1/s	0.30	0.39	0.51	0.65	0.72	0.83	1.03	0.40	0.48	0.65	0.77	0.92	1.04	1.19
RV CSSR, 1/s	-0.40	-0.45	-0.51	-0.58	-0.70	-0.79	-0.94	-0.35	-0.42	-0.51	-0.61	-0.70	-0.82	-1.10

CDSR, circumferential early diastolic strain rate; CSSR, circumferential peak systolic strain rate; LDSR, longitudinal early diastolic strain rate; LSSR, longitudinal peak systolic strain rate; LV, left ventricle; RDSR, radial early diastolic strain rate; RSSR, radial peak systolic strain rate; RV, right ventricle

Table S3. Cardiovascular magnetic resonance myocardial tagging-derived strain rate reference percentiles in adolescents.

	BOYS							GIRLS						
	Percentiles							Percentiles						
	3	10	25	50	75	90	97	3	10	25	50	75	90	97
Myocardial tagging														
LV LDSR, 1/s	0.24	0.37	0.43	0.62	0.77	0.85	0.98	0.33	0.44	0.55	0.68	0.86	0.97	1.07
LV LSSR, 1/s	-0.65	-0.72	-0.77	-0.82	-0.90	-0.94	-1.02	-0.68	-0.76	-0.80	-0.84	-0.92	-0.99	-1.15
LV CDSR, 1/s	0.80	0.90	0.97	1.05	1.15	1.29	1.50	0.63	0.99	1.05	1.16	1.26	1.35	1.43
LV CSSR, 1/s	-0.81	-0.88	-0.98	-1.05	-1.12	-1.22	-1.26	-0.80	-0.90	-0.97	-1.06	-1.13	-1.27	-1.33
LV RDSR, 1/s	-0.41	-0.64	-0.78	-0.95	-1.21	-1.44	-2.39	-0.30	-0.52	-0.63	-0.88	-0.98	-1.22	-1.42
LV RSSR, 1/s	0.85	0.99	1.11	1.33	1.47	1.58	1.87	0.67	0.85	0.98	1.14	1.36	1.49	1.84
LV Torsion, degrees/mm	0.05	0.13	0.18	0.22	0.24	0.27	0.31	0.12	0.14	0.20	0.23	0.29	0.36	0.41
RV LDSR, 1/s	0.33	0.71	0.88	0.97	1.07	1.16	1.29	0.46	0.53	0.83	0.97	1.12	1.18	1.28
RV LSSR, 1/s	-0.68	-0.76	-0.86	-0.95	-1.04	-1.15	-1.27	-0.58	-0.76	-0.87	-0.92	-0.98	-1.08	-1.10
RV CDSR, 1/s	0.44	0.54	0.63	0.74	0.86	0.99	1.08	0.42	0.47	0.64	0.74	0.85	0.94	1.01
RV CSSR, 1/s	-0.35	-0.57	-0.64	-0.71	-0.80	-0.88	-0.96	-0.51	-0.57	-0.63	-0.71	-0.77	-0.89	-0.91

CDSR, circumferential early diastolic strain rate; CSSR, circumferential peak systolic strain rate; LDSR, longitudinal early diastolic strain rate; LSSR, longitudinal peak systolic strain rate; LV, left ventricle; RDSR, radial early diastolic strain rate; RSSR, radial peak systolic strain rate; RV, right ventricle

Table S4. Absolute-agreement and consistency-of-agreement intraclass correlation coefficients (ICC) and their 95% confidence intervals (95%CI) for intraobserver comparisons of cardiovascular magnetic resonance-derived strain values.

Variable	n	Feature tracking		Myocardial tagging	
		Absolute (95% CI)	Consistency (95% CI)	Absolute (95% CI)	Consistency (95% CI)
LVLS, %	30	0.98 (0.93 to 0.99)	0.98 (0.96 to 0.99)	0.93 (0.69 to 0.98)	0.96 (0.91 to 0.98)
LVCS, %	30	0.91 (0.78 to 0.96)	0.92 (0.84 to 0.96)	0.93 (0.86 to 0.97)	0.94 (0.87 to 0.97)
LVRS, %	30	0.99 (0.98 to >0.99)	0.99 (0.98 to >0.99)	0.93 (0.87 to 0.97)	0.93 (0.86 to 0.97)
RVLS, %	30	0.91 (0.83 to 0.96)	0.91 (0.82 to 0.96)	0.89 (0.73 to 0.95)	0.91 (0.82 to 0.96)
RVCS, %	30	0.98 (0.95 to 0.99)	0.98 (0.95 to 0.99)	0.89 (0.64 to 0.96)	0.93 (0.85 to 0.96)

Values >0.99 are indicated as >0.99, not rounded to 1. CI, confidence interval; CS, circumferential strain; LS, longitudinal strain; LV, left ventricular; RS, radial strain; RV, right ventricular

Table S5. Absolute-agreement and consistency-of-agreement intraclass correlation coefficients (ICC) and their 95% confidence intervals (95%CI) for interobserver comparisons of cardiovascular magnetic resonance-derived strain values.

Variable	n	Feature tracking		Myocardial tagging	
		Absolute (95% CI)	Consistency (95% CI)	Absolute (95% CI)	Consistency (95% CI)
LVLS, %	30	0.96 (0.83 to 0.99)	0.98 (0.95 to 0.99)	0.93 (0.86 to 0.97)	0.93 (0.86 to 0.97)
LVCS, %	30	0.89 (0.55 to 0.96)	0.93 (0.85 to 0.96)	0.80 (0.43 to 0.92)	0.85 (0.72 to 0.93)
LVRS, %	30	0.98 (0.94 to 0.99)	0.99 (0.97 to 0.99)	0.67 (0.17 to 0.86)	0.77 (0.58 to 0.89)
RVLS, %	30	0.90 (0.81 to 0.95)	0.91 (0.82 to 0.96)	0.80 (0.38 to 0.92)	0.87 (0.74 to 0.93)
RVCS, %	30	0.83 (0.46 to 0.93)	0.88 (0.77 to 0.94)	0.82 (0.04 to 0.95)	0.92 (0.85 to 0.96)

CI, confidence interval; CS, circumferential strain; LS, longitudinal strain; LV, left ventricular; RS, radial strain; RV, right ventricular

Table S6. Bias and lower and upper limits of agreement from the Bland-Altman plots and their 95% confidence intervals (95%CI) for intraobserver comparisons of cardiovascular magnetic resonance-derived strain measurements

		Feature tracking			Myocardial tagging		
Variable	**n**	**Bias (95%CI)**	**LLA (95%CI)**	**ULA (95%CI)**	**Bias (95%CI)**	**LLA (95%CI)**	**ULA (95%CI)**
LVLS, %	30	0.2 (0.1 to 0.4)	-0.6 (-0.9 to -0.3)	1.1 (0.8 to 1.3)	0.4 (0.2 to 0.6)	-0.6 (-0.9 to -0.2)	1.4 (1.1 to 1.7)
LVCS, %	30	0.5 (0.1 to 0.9)	-1.5 (-2.2 to -0.8)	2.5 (1.9 to 3.2)	0.3 (-0.0 to 0.7)	-1.4 (-2.0 to -0.8)	2.1 (1.5 to 2.6)
LVRS, %	30	0.6 (0.1 to 1.1)	-2.0 (-2.8 to -1.1)	3.2 (2.3 to 4.0)	0.2 (-0.7 to 1.2)	-4.8 (-6.4 to -3.1)	5.2 (3.5 to 6.8)
RVLS, %	30	0.2 (-0.3 to 0.7)	-2.6 (-3.6 to -1.7)	3.0 (2.1 to 4.0)	0.7 (0.2 to 1.1)	-1.7 (-2.5 to -1.0)	3.1 (2.3 to 3.9)
RVCS, %	30	0.2 (-0.0 to 0.4)	-0.9 (-1.3 to -0.6)	1.2 (0.9 to 1.6)	0.7 (0.3 to 1.0)	-1.2 (-1.8 to -0.5)	2.5 (1.9 to 3.2)

CI, confidence interval; CS, circumferential strain; LLA, lower limit of agreement; LS, longitudinal strain; LV, left ventricular; RS, radial strain; RV, right ventricular; ULA, upper limit of agreement

Table S7. Bias and lower and upper limits of agreement from the Bland-Altman plots and their 95% confidence intervals (95%CI) for interobserver comparisons of cardiovascular magnetic resonance-derived strain measurements

		Feature Tracking			Tagging		
Variable	**n**	**Bias (95%CI)**	**LLA (95%CI)**	**ULA (95%CI)**	**Bias (95%CI)**	**LLA (95%CI)**	**ULA (95%CI)**
LVLS, %	30	-0.4 (-0.5 to -0.2)	-1.3 (-1.6 to -1.0)	0.5 (0.2 to 0.8)	-0.1 (-0.4 to 0.1)	-1.4 (-1.9 to 1.0)	1.2 (0.8 to 1.7)
LVCS, %	30	-0.8 (-1.2 to -0.4)	-2.7 (-3.4 to -2.1)	1.1 (0.5 to 1.7)	1.0 (0.5 to 1.6)	-1.8 (-2.7 to -0.8)	3.9 (2.9 to 4.8)
LVRS, %	30	-1.0 (-1.6 to -0.4)	-4.2 (-5.2 to -3.1)	2.2 (1.1 to 3.2)	4.0 (2.2 to 5.7)	-5.2 (-8.2 to -2.2)	13.1 (10.1 to 16.1)
RVLS, %	30	0.4 (-0.1 to 1.0)	-2.4 (-3.3 to -1.5)	3.2 (2.3 to 4.2)	1.2 (0.7 to 1.8)	-1.8 (-2.7 to -0.8)	4.2 (3.2 to 5.2)
RVCS, %	30	1.1 (0.6 to 1.7)	-1.7 (-2.7 to -0.8)	4.0 (3.0 to 4.9)	1.4 (1.0 to 1.8)	-0.6 (-1.3 to 0.0)	3.4 (2.7 to 4.1)

CI, confidence interval; CS, circumferential strain; LLA, lower limit of agreement; LS, longitudinal strain; LV, left ventricular; RS, radial strain; RV, right ventricular; ULA, upper limit of agreement